

Synthesis and Photophysical and Cation-Binding Properties of Mono- and Tetranaphthylcalix[4]arenes as Highly Sensitive and Selective Fluorescent Sensors for Sodium

Isabelle Leray,^{*,[a]} Jean-Pierre Lefevre,^[a, b] Jean-François Delouis,^[a] Jacques Delaire,^[a] and Bernard Valeur^{*,[a, b]}

Abstract: The syntheses and properties of two calixarene-based fluorescent molecular sensors are reported. These comprise *tert*-butylcalix[4]arene either with one appended fluorophore and three ester groups (Calix-AMN1), or with four appended fluorophores (Calix-AMN4). The fluorophore is 6-acyl-2-methoxynaphthalene (AMN), which contains an electron-donating substituent (methoxy group) conjugated to an electron-withdrawing substituent (carbonyl group); this allows photoinduced charge transfer (PCT) to occur upon excitation. The investigated fluoroionophores thus belong to the family of PCT fluorescent molecular sensors. In addition to the expected red shifts of the absorption and

emission spectra upon cation binding, a drastic enhancement of the fluorescence quantum yield—in an “off–on” fashion comparable to that seen in photoinduced electron transfer (PET) molecular sensors—was observed. For Calix-AMN1, it increases from 10^{-3} for the free ligand to 0.68 for the complex with Ca^{2+} . This exceptional behaviour can be interpreted in terms of the relative locations of the $n\pi^*$ and $\pi\pi^*$ levels, which depend on the charge density of the bound cation. For Calix-AMN4, in

Keywords: calixarenes • excimers • fluorescence spectroscopy • sensors • supramolecular chemistry

addition to the photophysical effects observed for Calix-AMN1, interactions between the chromophores by complexation with some cations have been found in the ground state (hypochromic effect) and in the excited state (excimer formation). Steady-state fluorescence anisotropy measurements for the system $\text{Na}^+ \subset \text{Calix-AMN4}$, show a depolarization effect due to energy transfer (homotransfer) between the fluorophores. Regarding the complexing properties, a high selectivity for Na^+ over K^+ , Li^+ , Ca^{2+} and Mg^{2+} was observed in ethanol and ethanol–water mixtures. The selectivity (Na^+ /other cations) expressed as the ratio of the stability constants was found to be more than 400.

Introduction

The design of selective fluorescent molecular sensors for cations is a subject of considerable interest because of their numerous potential applications in analytical chemistry, biology, medicine (clinical diagnosis), environmental chemistry, chemical oceanography etc.^[1–5] Most fluorescent molecular sensors consist of a cation recognition unit (ionophore) linked to a fluorophore; thus they are often called fluoro-

ionophores. The recognition moiety is responsible for the selectivity and the efficiency of binding, therefore considerable efforts have been made to develop selective sensors for particular cations. In this respect, calixarenes with appropriate appended groups exhibit high selectivities^[6] and have been shown to be useful building blocks in the design of fluorescent sensors for cations.^[7–12] The design of such calixarene-based sensors differs according to the nature of the cation and to the photoinduced process responsible for the photophysical changes upon cation binding: photoinduced electron transfer (PET),^[7] photoinduced charge transfer (PCT),^[8, 9] excimer formation^[10] or energy transfer.^[11]

It is worth bearing in mind that the electron-donor and electron-acceptor groups in PET sensors are nonconjugated (transfer of an electron), whereas those in PCT sensors are conjugated (partial charge transfer).

A distinct feature of PET molecular sensors is the very large cation-induced change in fluorescence intensity that is usually observed. The absence of a shift in the fluorescence or excitation spectra, however, precludes the possibility of intensity-ratio measurements at two wavelengths. In contrast,

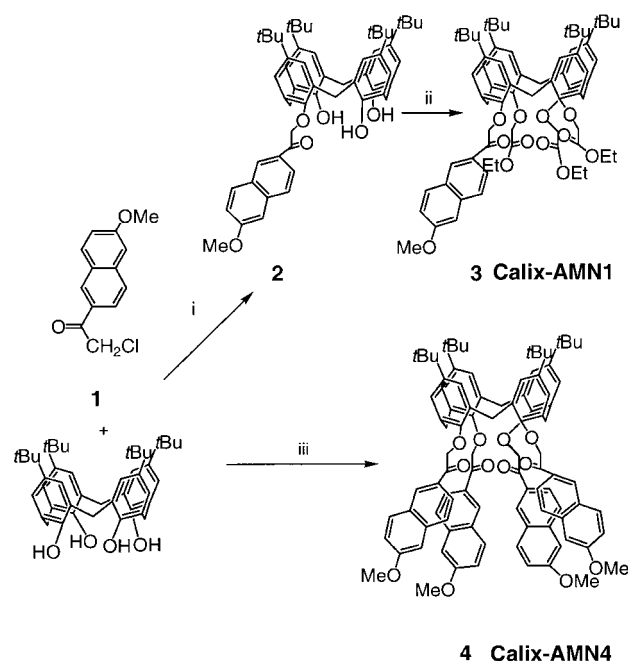
[a] Dr. I. Leray, Prof. B. Valeur, J.-P. Lefevre, J.-F. Delouis, Prof. J. Delaire
Laboratoire de Photophysique et Photochimie
Supramoléculaires et Macromoléculaires (CNRS UMR 8531)
Département de Chimie, ENS-Cachan
61 Avenue du Président Wilson
94235 Cachan cedex (France)
Fax: (+33)1-47-40-24-54
E-mail: icmleray@ppsm.ens-cachan.fr, valeur@cnam.fr

[b] Prof. B. Valeur, J.-P. Lefevre
Laboratoire de Chimie Générale
Conservatoire National des Arts et Métiers
292 rue Saint-Martin, 75141 Paris Cedex 3 (France)

shifts in the fluorescence or excitation spectra of PCT molecular sensors permit ratiometric measurements to be made; this allows the determination of cation concentration independently of various parameters such as sensor concentration, incident-light intensity and photobleaching. However, the changes in fluorescence quantum yield on cation binding are generally not very large relative to those observed with PET sensors. This paper reports the properties of two calixarene-based PCT molecular sensors that exhibit an enhancement of fluorescence quantum yield—in an “off-on” fashion—as large as those seen in PET sensors with the additional advantage of spectral shifts upon complexation.

In line with our previous works on PCT fluoroionophores,^[13] we selected 6-acyl-2-methoxynaphthalene (AMN) as a fluorophore. This moiety incorporates an electron-donating substituent (methoxy group) conjugated with an electron-withdrawing substituent (carbonyl group). As regards the recognition moiety,^[14] a *tert*-butylcalix[4]arene frame with appended carbonyl groups was chosen, with the aim of selectivity for sodium. The investigated fluoroionophores—Calix-AMN1 and Calix-AMN4, comprising *tert*-butylcalix[4]arene with one and four appended acyl naphtha-

lene fluorophores, respectively—are shown in Scheme 1. Preliminary results on Calix-AMN1 have been reported previously.^[9]



Scheme 1. Synthesis of Calix-AMN1 (3) and Calix-AMN4 (4): i) KHCO_3 , acetone; ii) $\text{BrCH}_2\text{COOEt}$, K_2CO_3 , acetone; iii) NaI , K_2CO_3 , acetone.

Abstract in French: Cet article présente la synthèse et l'étude des propriétés photophysiques et de complexation de deux nouvelles sondes fluorescentes à base de calixarène. Ces fluoroionophores sont constitués de *tert*-butylcalix[4]arènes liés de façon covalente à un fluorophore et trois groupes ester (Calix-AMN1) ou à quatre fluorophores (Calix-AMN4). Le fluorophore utilisé est composé d'un groupe méthoxy (donneur) conjugué à un groupe carbonyle (accepteur), participant à la complexation du cation. Ainsi un transfert de charge photoinduit se produit lors de l'excitation lumineuse. La complexation du cation par le calixarène s'accompagne non seulement d'un déplacement bathochrome des spectres d'absorption et de fluorescence mais aussi d'une très forte augmentation du rendement quantique de fluorescence aussi importante que dans le cas de fluorionophores fonctionnant suivant le principe du transfert d'électron photoinduit (PET). Dans le cas du Calix-AMN1, le rendement quantique passe de $\approx 10^{-3}$ à 0.68 lors de la complexation avec le calcium. Ce phénomène remarquable peut s'expliquer par une modification des niveaux d'énergie relatifs des états singulets $\pi\pi^*$ et $n\pi^*$ (dépendant de la densité de charge du cation complexé). Dans le cas du Calix-AMN4, des interactions entre les chromophores lors de la complexation de cations ont été mises en évidence aussi bien à l'état fondamental (effet hypochrome) qu'à l'état excité (formation d'excimères). D'autre part des mesures d'anisotropie de fluorescence sur le système $\text{Na}^+ \subset \text{Calix-AMN4}$ ont montré un effet de dépolarisation dû à l'existence d'un transfert d'énergie entre les chromophores (homotransfert). En ce qui concerne les propriétés de complexation, une excellente sélectivité de ces systèmes vis-à-vis du sodium par rapport aux autres cations a été obtenue dans des solvants protiques (éthanol et mélanges éthanol–eau). La sélectivité du sodium par rapport aux autres cations (exprimée par le rapport des constantes de stabilité) est supérieure à 400.

The new Calix-AMN4 compound, containing four fluorophores, offers additional interesting features with respect to Calix-AMN1 in terms of: i) sensitivity of detection (molar absorption coefficient four times larger), ii) additional photophysical effects (possibility of excimer formation) and iii) improved photochemical stability. The advantages of multi-chromophoric sensors have already been outlined, in particular for sensors based on dendrimers.^[15]

In this paper the syntheses of Calix-AMN1 and Calix-AMN4 are reported, together with their cation-induced photophysical changes and their complexing properties.

Results and Discussion

Synthesis: Calix-AMN1 (3) was prepared (Scheme 1) from the parent calix[4]arene. 4-*tert*-Butylcalix[4]arene was mono-alkylated with 2-chloroacetyl-6-methoxynaphthalene in the presence of KHCO_3 in acetone. The 2-chloroacetyl-6-methoxynaphthalene was obtained by Friedel–Crafts acylation of methoxynaphthalene with chloroacetyl chloride in nitrobenzene.^[16] The remaining three phenolic positions were then functionalized with ethyl bromoacetate in acetone in the presence of K_2CO_3 .

Calix-AMN4 (4) was prepared according to Scheme 1, by condensation with 2-chloroacetyl-6-methoxynaphthalene and K_2CO_3 in acetone^[14] in the presence of sodium iodide to provide halogen exchange.

Compounds 2, Calix-AMN1 and Calix-AMN4 had ^1H NMR spectra characteristic^[6] of a cone conformation.

Results of the photophysical studies

Absorption spectra: Figure 1 displays the absorption spectra of Calix-AMN1 and Calix-AMN4 in acetonitrile. In the free ligands, the molar absorption coefficient of Calix-AMN4 is about four times larger than that of Calix-AMN1; this implies

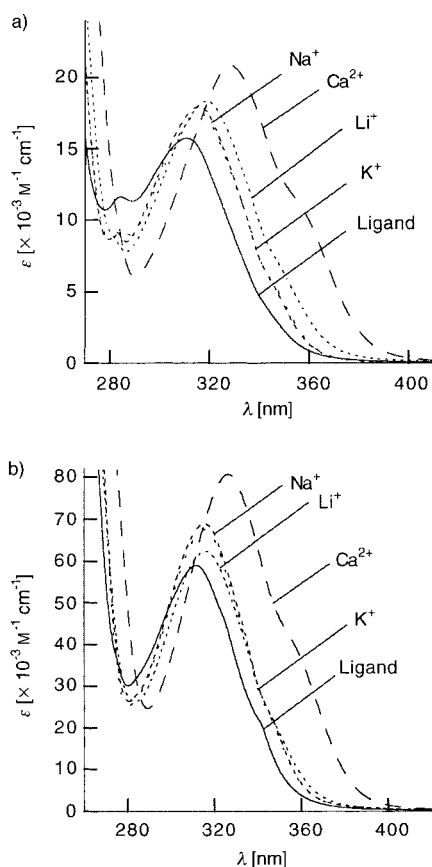


Figure 1. Absorption of a) Calix-AMN1 and b) Calix-AMN4 in acetonitrile and their complexes with perchlorate salts.

that there is no significant interaction between the naphthalene fluorophores in the ground state. Upon cation binding, the observed red shifts in the absorption spectra of Calix-AMN1 and Calix-AMN4 were to be expected from cation–dipole interactions: the interaction between the bound cation and the electron-withdrawing carbonyl group conjugated to the electron-donating methoxy group. These effects on absorption spectra are comparable to those reported with aminocoumarins linked to crown ethers.^[13]

After division of the absorption coefficients of the Calix-AMN4 complexes by four, for comparison with those of the Calix-AMN1 complexes, no significant difference was observed except with lithium complexes, for which a hypochromic effect of about 15% was found on going from the complex $\text{Li}^+ \subset \text{Calix-AMN1}$ to the complex $\text{Li}^+ \subset \text{Calix-AMN4}$. This can be explained by the smaller size of the lithium cation, the binding of which reduces the distance between the naphthalene rings so that some excitonic coupling takes place. This was confirmed by energy-minimized structures (Figure 2) obtained according to the procedure described by Diamond for similar compounds.^[17] The estimated interatomic distances

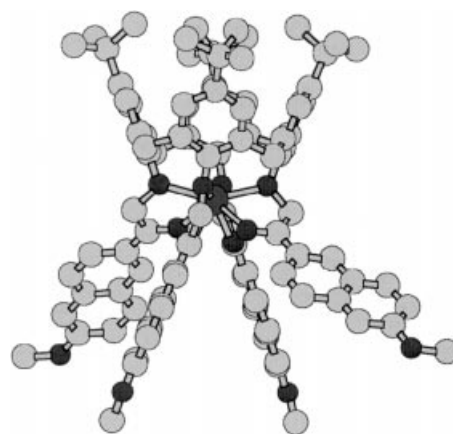


Figure 2. Energy-minimized structure of $\text{Na}^+ \subset \text{Calix-AMN4}$ obtained by using Hyperchem software with the molecular mechanics subroutine.

between similar pairs of atoms depends on the bound cation. The average distance between the carbonyl groups of the naphthalene rings decreases in the following order: 0.57 nm for the complex of Calix-AMN4 with K^+ , 0.53 nm for Ca^{2+} , 0.51 nm for Na^+ and 0.48 nm for Li^+ .

Fluorescence spectra and quantum yields: The emission spectra of Calix-AMN1 and Calix-AMN4 and their complexes in acetonitrile are presented in Figure 3. The two ligands have very low fluorescence quantum yields ($\approx 10^{-3}$).

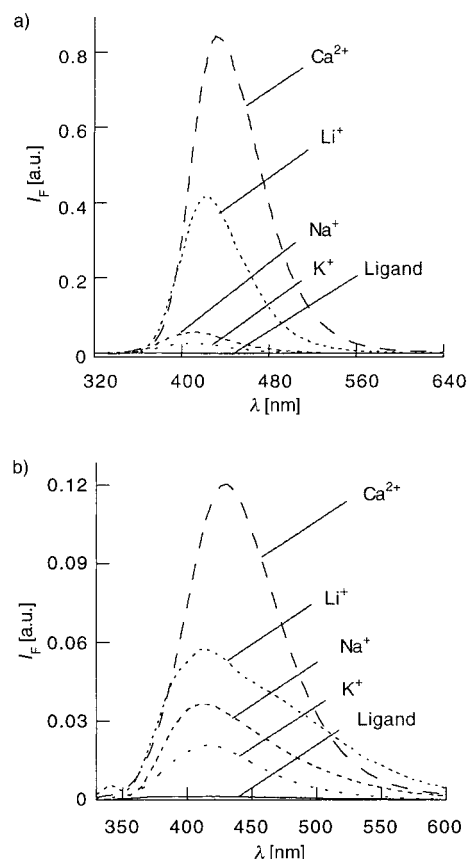


Figure 3. Corrected emission spectra of a) Calix-AMN1 and b) Calix-AMN4 and their complexes with perchlorate salts in acetonitrile.

Interaction of a cation with the carbonyl group of the fluorophore produces a red shift in the emission spectrum, as a result of the enhancement of the photoinduced charge transfer from the methoxy group to the carbonyl group. Moreover, an outstanding enhancement of the fluorescence quantum yield was observed (0.68 for the complex $\text{Ca}^{2+} \subset \text{Calix-AMN1}$).

For the complexes $\text{Ca}^{2+} \subset \text{Calix-AMN4}$ and $\text{Li}^+ \subset \text{Calix-AMN4}$, the fluorescence quantum yields were found to be smaller than those of the corresponding Calix-AMN1 complexes as a result of self-quenching of the fluorophores. In addition to this effect, tails at long wavelengths were observed in the emission spectra of the complexes with Li^+ and Na^+ . This is likely to be due to excimer formation between adjacent naphthalene groups, previously observed in the case of β -cyclodextrins with seven appended naphthalene chromophores.^[18] The relative contributions of excimers and monomers to the fluorescence intensities were found to be related to the size of the complexed cation ($\text{Li}^+ > \text{Na}^+ > \text{K}^+$). The smaller the size of the cation, the smaller the average distance between the naphthalene groups and the higher the probability of excimer formation. This result is in accordance with the ground-state interaction between the fluorophores in the complex $\text{Li}^+ \subset \text{Calix-AMN4}$, as revealed by the absorption spectrum (hypochromic effect).

In ethanol, the enhancements of the fluorescence quantum yields of Calix-AMN1 and Calix-AMN4 upon complexation with Na^+ and K^+ follow the same trend as in acetonitrile. Measurement of the fluorescence quantum yields of complexes of Calix-AMN4 and Calix-AMN1 with the other cations (Li^+ , Ca^{2+}) in ethanol was impossible because of the very small stability constants (see below).

Time-resolved fluorescence: An attempt to record the fluorescence decay of free Calix-AMN1 failed because of its very low fluorescence quantum yield. The fluorescence decay curves of complexes of Calix-AMN1 with various cations are shown in Figure 4a. Table 1 shows that in most cases a sum of two or three exponentials was necessary to obtain a satisfactory fit of the decays. Such multiexponential decays can be interpreted in terms of the existence of different types of available binding sites for the complex. Indeed, different binding sites were found by Arnaud-Neu et al.^[14] by X-ray diffraction on samples of tetraethyl *p*-*tert*-butylcalix[4]arene-tetraacetate. Interestingly, in the case of the complex with Ca^{2+} , the fluorescence decay was found to be almost monoexponential; this led us to conclude that there is close to a single conformer for this complex. The average decay times (defined as $\langle \tau \rangle = \sum f_i \tau_i$, in which f_i and τ_i are the fractional intensities and time constants, respectively) for the complexes follow the variation in the fluorescence quantum yields.

The fluorescent decays for the complexes of Calix-AMN4 with alkali and alkaline earth cations were recorded at two observation wavelengths: at 420 nm (Figure 4b), where no emission from the excimers was expected, and at 520 nm, which should provide the larger contribution. A sum of two or three exponentials was necessary to fit the fluorescence decays. Compared with Calix-AMN1 complexes, the fluorescence decays of the Calix-AMN4 counterparts also reflect

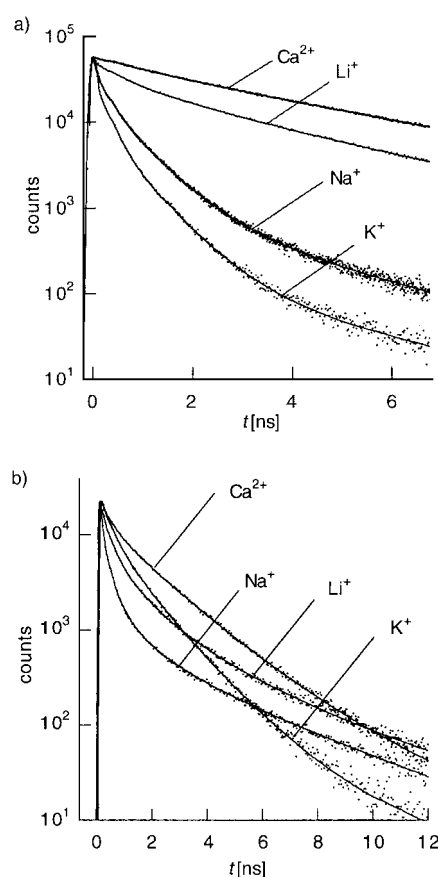


Figure 4. a) Fluorescence decays of Calix-AMN1 complexes in acetonitrile. Excitation wavelength 310 nm, emission wavelength 420 nm; b) fluorescence decays of Calix-AMN4 complexes with perchlorate salts in acetonitrile. Excitation wavelength 310 nm, emission wavelength 420 nm.

Table 1. Fluorescent decay components [ns] of the various complexes with perchlorate salts of Calix-AMN1 and Calix-AMN4 in acetonitrile at different observation wavelengths [$\lambda_{\text{exc}} = 310 \text{ nm}$]

	λ_{em} [nm]	τ_1 [ns] (f_1)	τ_2 [ns] (f_2)	τ_3 [ns] (f_3)	$\langle \tau \rangle$ [ns]	χ^2_{R}
Calix-AMN1						
K ⁺	420	0.19 ± 0.02	0.67 ± 0.02	3.0 ± 0.5	0.51	1.1
		(0.52 ± 0.06)	(0.44 ± 0.05)	(0.04 ± 0.04)		
		(0.28 ± 0.02)	(0.58 ± 0.03)	(0.14 ± 0.12)		
Na ⁺	420	0.22 ± 0.01	0.71 ± 0.01	2.9 ± 0.5	0.81	1.1
		(0.33 ± 0.05)	1.03 ± 0.06	3.37 ± 0.02		
Li ⁺	420	0.33 ± 0.05	1.03 ± 0.06	3.37 ± 0.02	2.8	1.03
		(0.05 ± 0.02)	(0.16 ± 0.04)	(0.78 ± 0.04)		
Ca ²⁺	420		1.0 ± 0.26	4 ± 0.15	3.8	1.05
			(0.05 ± 0.03)	(0.94 ± 0.02)		
Calix-AMN4						
K ⁺	420	0.27 ± 0.03	1.13 ± 0.06		0.9	1.07
		(0.22 ± 0.06)	(0.73 ± 0.05)			
Na ⁺	520		1.48 ± 0.03		1.5	0.96
Na ⁺	420	0.33 ± 0.04	1 ± 0.3	3.4 ± 0.5	1.7	1.07
		(0.31 ± 0.07)	(0.29 ± 0.1)	(0.4 ± 0.1)		
Li ⁺	520		1.3 ± 0.2	3.6 ± 0.2	3.2	1.03
			(0.18 ± 0.07)	(0.81 ± 0.6)		
Li ⁺	420	0.21 ± 0.02	0.90 ± 0.10	2.9 ± 0.5	1.2	1.01
		(0.25 ± 0.05)	(0.36 ± 0.08)	(0.3 ± 0.1)		
Ca ²⁺	520		1.5 ± 0.2	4.6 ± 0.3	4.0	0.97
			(0.82 ± 0.04)	(0.17 ± 0.05)		
Ca ²⁺	420	0.27 ± 0.02	1.64 ± 0.05		1.4	0.99
		(0.16 ± 0.03)	(0.84 ± 0.03)			
Ca ²⁺	520		1.96 ± 0.01	15.2 ± 1.4	3.3	1.03
			(0.9 ± 0.01)	(0.1 ± 0.03)		

interactions between the fluorophores. In particular, the decays are affected by the formation of excimers, especially for smaller cations. However, it is important to note that no rise time resulting from excimer formation was detected at 520 nm on the shortest timescale available through our instrumentation (around 60 ps); this means that the excimers are preformed, as previously reported for β -cyclodextrins with seven appended naphthalenic fluorophores.^[18]

Interpretation of the fluorescence enhancement upon cation binding: In order to understand the enhancement of the fluorescence quantum yield upon complexation, the relative locations of the singlet $n\pi^*$ and $\pi\pi^*$ states of the naphthalene fluorophores in the absence and in the presence of a bound cation should be considered. This fluorophore, belonging to the family of ketones, would indeed be expected to have a low-lying $n\pi^*$ excited state.^[19] The molar absorption coefficient of an $n\pi^*$ band is generally of the order of $10^2 \text{ M}^{-1} \text{ cm}^{-1}$. Therefore, in view of the absorption spectrum and the molar absorption coefficient ($\approx 10^4 \text{ M}^{-1} \text{ cm}^{-1}$), the $n\pi^*$ absorption band is likely to be buried beneath the intense $\pi\pi^*$ absorption band generally observed for aromatic ketones. The very low fluorescence quantum yield of Calix-AMN1 can be explained in terms of efficient intersystem crossing from the low-lying $n\pi^*$ excited state to the triplet state, which has a $\pi\pi^*$ character, as previously determined by ESR for 6-methoxy-2-acetonaphthalene.^[20]

It is worth noting that the fluorescence quantum yield, the absorption spectra and the emission spectra of Calix-AMN1 are solvent-dependent. In ethanol, the fluorescence quantum yield is twice as large as in acetonitrile. The greater the polarity of the solvent, the higher the fluorescence quantum yield. This observation is consistent with the fact that, in general, when the polarity and the hydrogen-bonding power of the solvent increases, the $n\pi^*$ state shifts to higher energy whereas the $\pi\pi^*$ state shifts to lower energy and can eventually become the low-lying excited state, with the consequence of a higher fluorescence quantum yield (see, for instance, the solvent-dependence of the luminescence of xanthone.^[21])

Possible changes in the relative locations of the $n\pi^*$ and $\pi\pi^*$ levels as a function of solvent polarity should be kept in mind when the effect of cation binding on the fluorescence quantum yield of Calix-AMN1 is considered. Such an analogy is indeed supported by the fact that the higher the charge density of the bound cation (Li^+ and Ca^{2+}), the larger the fluorescence quantum yield (Figure 3). Therefore, it is reasonable to make the assumption that interaction with a bound cation can reduce the energy difference between the $n\pi^*$ and $\pi\pi^*$ levels and can even invert these levels if the charge density on the cation is large enough. When the $n\pi^*$ and $\pi\pi^*$ levels are close (in cases of interaction with cations of moderate charge density, such as Na^+ and K^+), there is competition between intersystem crossing from the $n\pi^*$ state and emission from the $\pi\pi^*$ state (allowed transition). In the case of cations of greater charge density, de-excitation mainly occurs from the $\pi\pi^*$ state through the allowed $S_1 \rightarrow S_0$ transition, and the fluorescence quantum yield is higher.

These observations prompted us to examine the radiative and nonradiative rate constants (k_r and $k_{nr} = k_{ic} + k_{isc}$ respectively) for de-excitation of the low-lying S_1 states. These can be calculated from the fluorescence quantum yields and average excited-state lifetimes for the complexes of Calix-AMN1 and Calix-AMN4 (Table 2). Since the fluorescence

Table 2. Photophysical properties for Calix-AMN1 and Calix-AMN4 and their complexes with perchlorate salts in acetonitrile

	Charge density [q \AA^{-1}]	Φ_F	$\langle \tau \rangle$ [ns]	k_r [10^8 s^{-1}]	$k_{nr} = k_{ic} + k_{isc}$ [10^8 s^{-1}]
Calix-AMN1		0.001			
K^+	0.75	0.020	0.5	0.4	19.6
Na^+	1.03	0.044	0.8	0.5	12
Li^+	1.47	0.32	2.8	1.14	2.4
Ca^{2+}	2.02	0.68	3.8	1.78	0.84
Calix-AMN4		0.001			
K^+	0.75	0.024	0.9	0.27	10.8
Na^+	1.03	0.031	1.7	0.18	5.7
Li^+	1.47	0.059	1.2	0.49	7.9
Ca^{2+}	2.02	0.092	1.4	0.66	6.5

decays deviate strongly from a single exponential in most cases, the values of these rate constants should be taken with caution, but the trends provide valuable information. For the complexes with Calix-AMN1, the nonradiative rate constant decreases drastically when the charge density of the bound cation increases; it varies from about $2 \times 10^9 \text{ s}^{-1}$ for $\text{K}^+ \subset \text{Calix-AMN1}$ to $8.4 \times 10^7 \text{ s}^{-1}$ for $\text{Ca}^{2+} \subset \text{Calix-AMN1}$. Such a drastic change is consistent with a decrease in the efficiency of intersystem crossing as a de-excitation pathway as the charge density of the cation increases. This supports our interpretation in terms of the relative locations of the singlet $n\pi^*$ and $\pi\pi^*$ states, the latter becoming the low-lying state in the presence of cations of large charge density.

In order to confirm this interpretation further, the transient absorption spectra of Calix-AMN1 and its complexes with alkali and alkaline earth cations were recorded in acetonitrile after nanosecond pulse excitation at 355 nm (Figure 5). The triplet absorption spectrum of the free ligand exhibits a maximum at 447 nm (Table 3). For the complex $\text{Ca}^{2+} \subset \text{Calix-AMN1}$, the triplet absorption was too low to be determined at

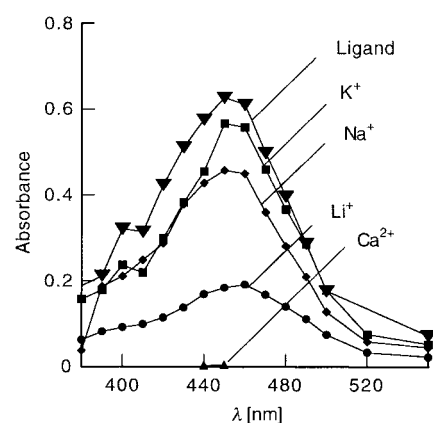


Figure 5. Transient absorption spectra of Calix-AMN1 and its complexes in degassed acetonitrile obtained 8 ns after laser pulse excitation at 355 nm.

Table 3. Transient absorption maxima and triplet lifetimes of Calix-AMN1 and its complexes with perchlorate salts in acetonitrile.

Cation	Diameter [Å]	Charge density [q Å ⁻¹]	λ_T [nm]	τ_T [μs]
Calix-AMN1			447	1.37
K ⁺	2.66	0.75	450	4.14
Na ⁺	1.94	1.03	450	4.83
Li ⁺	1.36	1.47	456	10
Ca ²⁺	1.98	2.02	not measurable	

each wavelength. For the complexes with the other cations, the triplet absorption efficiencies were found to be smaller than those of the ligands. This effect is again related to the charge density of the bound cation and is in agreement with less-efficient intersystem crossing to the triplet state when the calixarene is complexed with a cation. The absence of a significant shift of the transient absorption spectra upon complexation (Table 3) means that the nature of the triplet state is the same whatever the bound cation and should have a $\pi\pi^*$ character according to El Sayed's rules.^[19] This is consistent with the ESR measurements on 6-methoxy-2-acetonaphthalene.^[20]

Finally, the single-exponential decays of the transient absorption show that the triplet lifetime increases when the charge density of the bound cation increases (Table 3). The nonradiative de-excitation from the triplet state indeed becomes slower when the spin–orbit coupling between the triplet state ($^3\pi\pi^*$ character, totally symmetrical) and the ground state (totally symmetrical) is weaker. Such an increase in the lifetime of the triplet states of aryl ketones on going from a $^3n\pi^*$ to a $^3\pi\pi^*$ triplet state has been described previously.^[22, 23]

In the case of Calix-AMN4, the interpretation of the calculated values for the nonradiative rate constants is not straightforward because of the additional excited state interactions between the fluorophores and excimer formation.

Steady-state fluorescence anisotropy: Since the fluorescence quantum yields of the free ligands, Calix-AMN1 and Calix-AMN4, are too low for it to be possible to carry out fluorescence polarization experiments, we compared the excitation polarization spectra of the sodium complexes of Calix-AMN1 and Calix-AMN4 in rigid glasses formed at 100 K from ethanol–methanol mixtures (9:1, v/v) (Figure 6). It turned out to be impossible to perform the same measurements for the complexes of Calix-AMN4 and Calix-AMN1 with the other cations (Li⁺, Ca²⁺, K⁺) because of their very low stability constants in ethanol (see below).

The anisotropy values of Calix-AMN4 are clearly smaller than those of Calix-AMN1, except upon excitation at the red edge of the absorption spectrum. Since rotational motions of the fluorophores are impossible in frozen glasses, this depolarization effect is solely due to nonradiative energy transfer between the fluorophores. Energy transfer was indeed expected, because the average distance between the fluorophores is about 0.51 nm, which is smaller than the Förster critical radius, estimated at about 0.8 nm (see

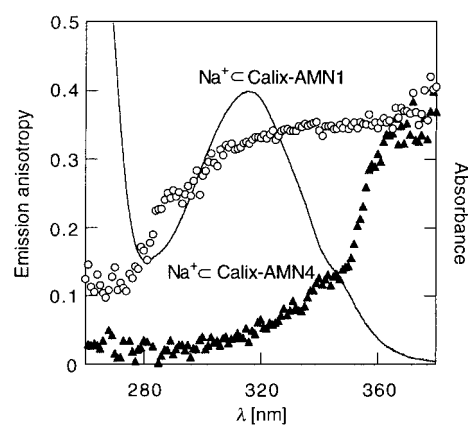


Figure 6. Excitation polarization spectra of the sodium complexes of Calix-AMN1 and Calix-AMN4 in rigid glasses formed from ethanol–methanol mixtures (9:1, v/v) at 100 K. Observation wavelength 410 nm.

Experimental Section). The lack of depolarization observed at the extreme red edge of the absorption spectrum (Weber red-edge effect) is due to inhomogeneous broadening, as previously reported with multichromophoric β -cyclodextrins.^[18, 24] It is interesting to note that the shoulder of the absorption spectrum at about 345 nm corresponds to a shoulder in the excitation polarization spectrum of Na⁺ ⊂ Calix-AMN4; this means that excitation at the red edge of vibronic bands is able to produce a vibronic red-edge effect (as in the case of multichromophoric cyclodextrins^[18, 24]).

Around the absorption maximum (≈ 315 nm), and thus in a region where red-edge effects should not be significant, the anisotropy value of Na⁺ ⊂ Calix-AMN1 is about 0.33 and that of Na⁺ ⊂ Calix-AMN4 is about 0.05–0.04. The ratio is thus about 7. This value should be compared with the value that would be observed if the fluorophores were oriented at random. In such a case, under the reasonable assumption that the energy-transfer process is very fast with respect to the fluorescence decay, the ratio should be 4, because there are four fluorophores. In fact, when the fluorophores are randomly oriented, only the initially excited one contributes significantly to the value of the anisotropy and, since the probability that this fluorophore emits a photon is 0.25, the anisotropy should be a quarter of the value in the absence of transfer. A ratio of 7 instead of 4 means that the fluorophores are not randomly oriented in the Na⁺ ⊂ Calix-AMN4 complex; in other words, the bound cation induces some preferential conformations, as expected.

Cation binding properties of Calix-AMN1 and Calix-AMN4:

The stoichiometries and stability constants of complexes were determined by analysis of the variations in absorbance or fluorescence intensity upon addition of metal ion. When the stoichiometry is 1:1, satisfactory fits must be obtained by using Equation (1) as previously reported.^[13b]

$$X = X_0 + \frac{X_{\text{lim}} - X_0}{2 C_L} \left[C_L + C_M + \frac{1}{\beta} - \sqrt{\left(C_L + C_M + \frac{1}{\beta} \right)^2 - 4 C_L C_M} \right] \quad (1)$$

Here X is the absorbance or fluorescence intensity of the solution. X_0 and X_{lim} are the values of X for the free ligand and the ML complex, respectively. C_L and C_M are the total

concentrations of ligand and metal ion, respectively, and β is the stability constant. When X_{lim} cannot be accurately determined, it can be left as a floating parameter in the analysis. An example of the spectral evolution and titration curve is given in Figure 7. Apart from the complexation of Calix-AMN1 with Na^+ in ethanol, satisfactory fits for 1:1 complexes were found.

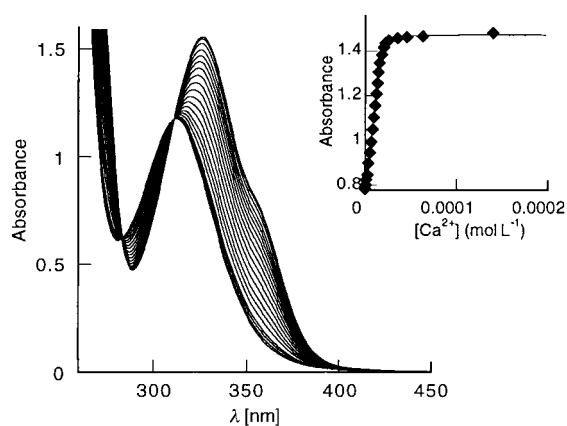
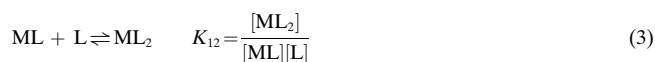


Figure 7. Evolution of the absorption spectrum of Calix-AMN4 ($1.9 \times 10^{-3} \text{ mol L}^{-1}$) upon addition of calcium perchlorate in acetonitrile. Inset: titration curve at 326 nm.

In the case of the complex of Calix-AMN1 with Na^+ in ethanol, no satisfactory fits were found by using Equation (1). Further analysis of the evolution of the whole absorption spectra (200 wavelengths) by means of the SPECFIT software (global analysis) showed that the titration curves were consistent with the formation of two complexes, metal/ligand 1:1 and 1:2; this is consistent with the NMR study undertaken by Detellier^[25] in the case of the complex of sodium with calix[4]arene tetraester. The constants of the successive equilibria K_{11} and K_{12} were determined.



The global equilibrium for the formation of the complex ML_2 is:



The stability constants obtained for the complexes with alkali and alkaline-earth cations in acetonitrile, ethanol and

water–ethanol mixtures are reported in Table 4. The values of the stability constants in acetonitrile are in good agreement with those previously reported in the case of tetraethyl *p*-tert-butylcalix[4]arenetetraacetate and *p*-tert-butylcalix[4]arene tetraphenyltraketone.^[14] In ethanol, the stability constants of the complexes with Na^+ and K^+ are much larger than those with Li^+ , Ca^{2+} and Mg^{2+} because the last three cations have higher charge densities and are thus more solvated than complexed, in contrast to the situation observed in acetonitrile. In ethanol, a good selectivity for Na^+ in preference to K^+ was observed. With the goal of practical applications, the stability constants were measured in the presence of water. Since the compounds Calix-AMN1 and Calix-AMN4 are not soluble in water, the stability constants were measured in ethanol–water mixtures. The maximum water content allowing sufficient solubility for spectroscopic measurements was 40% by volume for Calix-AMN1 and 20% by volume for Calix-AMN4. This fact is not a drawback because our goal is to design an optical-fibre device in which the fluoroionophores will be immobilized within a polymer or a sol-gel film. Insolubility in water is therefore preferable, to minimize leaching. The stability constants for Calix-AMN4 and Calix-AMN1 in an ethanol–water mixture (80:20, v/v) showed the expected very good selectivity towards sodium: the Na^+/K^+ selectivities (expressed by the ratio of the stability constants) were found to be 500 for Calix-AMN1 and 407 for Calix-AMN4. For Calix-AMN1, when the amount of water increases (EtOH/ H_2O 60:40, v/v), a very high selectivity towards sodium (1300) is still shown.

Conclusion

The fluoroionophores Calix-AMN1 and Calix-AMN4 described in the present paper belong to the PCT sensor class. It is remarkable that, in addition to the spectral shifts upon cation binding, they exhibit fluorescence enhancements as large as those found in PET sensors, due to inversion of the low-lying $\pi\pi^*$ and $\pi\pi^*$ levels. This is the first time that advantage has been taken of such a photophysical effect in a fluoroionophore. In addition to these outstanding photophysical responses, they show very good selectivities for sodium ions in water–ethanol mixtures. Such selectivities in the presence of water are very promising for practical applications to aqueous samples.

Table 4. Stability constants of Calix-AMN1 and Calix-AMN4 complexes with alkali and alkaline-earth cations in acetonitrile, ethanol and ethanol-water mixtures. The values given in this table are $\log_{10}\beta$.

Solvent	Compound	Li^+ (1.36 Å)	Na^+ (1.94 Å)	K^+ (2.66 Å)	Mg^{2+} (1.32 Å)	Ca^{2+} (1.98 Å)
acetonitrile	Calix-AMN1	6.28 ± 0.06	6.32 ± 0.07	4.74 ± 0.03	2.06 ± 0.04	5.3 ± 0.06
	Calix-AMN4	7.12 ± 0.12	7.03 ± 0.1	4.0 ± 0.01	2.75 ± 0.04	6.84 ± 0.12
ethanol	Calix-AMN1	0.9 ± 0.08	$\log K_{11} = 4.6 \pm 0.1$	2.87 ± 0.03	1.82 ± 0.06	1.25 ± 0.03
			$\log \beta_{12} = 9.7 \pm 0.13$			
			$\log K_{12} = 5.1 \pm 0.1$			
EtOH/ H_2O (80:20, v/v)	Calix-AMN1		3.87 ± 0.05	1.17 ± 0.05		
	Calix-AMN4	< 1	4.23 ± 0.04	1.62 ± 0.03	< 1	1.1 ± 0.03
EtOH/ H_2O (60:40, v/v)	Calix-AMN1		3.04 ± 0.07	0 ($\beta = 0.75 \pm 0.3$)		

Experimental Section

Synthesis

General procedures: ¹H and ¹³C NMR spectra were recorded at room temperature on a Bruker AC400 spectrometer. Elemental analyses were performed at the Institut des Chimie des Substances Naturelles (France).

2-Chloro-1-(6-methoxynaphthalen-2-yl)ethanone (1): 2-Methoxynaphthalene (3.95 g, 25 mmol) dissolved in nitrobenzene (20 ml) was added to a mixture of chloroacetyl chloride (2 mL, 25 mmol) and aluminium chloride (3.6 g, 27 mmol) in nitrobenzene (20 mL). The solution was left stirring at 0 °C for 20 min and was then heated at 40 °C for 2 h. Water was carefully added to the solution mixture. Nitrobenzene was removed by steam distillation. The product was extracted with ether. The organic layer obtained was washed with water, dried over MgSO₄ and evaporated in vacuum. Column chromatography on silica (eluent cyclohexane/AcOEt 95:5) gave a white solid, which was recrystallized from toluene/hexane to give 6-chloroacetyl-2-methoxynaphthalene (**1**). Yield: 1.28 g, 21%; m.p. 113 °C; ¹H NMR (400 MHz, CDCl₃): δ = 3.97 (s, 3H; CH₃), 4.84 (s, 2H; CH₂), 7.19 (m, 2H; ArH), 7.84 (m, 3H; ArH), 8.41 (s, 1H; ArH), elemental analysis calcd (%) for C₁₃H₁₁ClO₂: C 66.53, H 4.72; found C 66.53, H 4.73.

5,11,17,23-Tetra-tert-butyl-25-mono-[(6'-methoxynaphthalen-2'-yl)-carbonylmethoxy]calix[4]arene (2): 4-tert-Butylcalix[4]arene (414 mg, 0.63 mmol) was suspended in acetone (30 mL) containing KHCO₃ (126 mg, 1.26 mmol) and 2-chloro-1-(6-methoxynaphthalen-2-yl)ethanone (**1**) (300 mg, 1.26 mmol). The reaction mixture was heated under reflux for 2 days. The cooled mixture was filtrated and evaporated under reduce pressure. The crude product was chromatographed on silica column (eluent cyclohexane/AcOEt 95:5) to give **2**. Yield: 265 mg, 50.2%; m.p. 235 °C; ¹H NMR (400 MHz, CDCl₃): δ = 1.22 (s, 18H; tBu), 1.24 (s, 18H; tBu), 3.42 (d, ²J(H,H) = 13.6 Hz, 2H; Ar-αCH_{eq}), 3.45 (d, ²J(H,H) = 13 Hz, 2H; Ar-αCH_{eq}), 3.97 (s, 3H; CH₃), 4.32 (d, ²J(H,H) = 13.6 Hz, 2H; Ar-αCH_{eq}), 4.61 (d, ²J(H,H) = 13 Hz, 2H; Ar-αCH_{eq}), 5.76 (s, 2H; Ar-αCH₂), 7.1 (m, 10H; ArH), 7.84 (d, ²J(H,H) = 9 Hz, 1H; ArH), 7.88 (d, ²J(H,H) = 9.3 Hz, 1H; ArH), 8.06 (d, ²J(H,H) = 8.5 Hz, 1H; ArH), 8.46 (s, 1H; ArH), 9.55 (s, 2H; OH), 10.38 (s, 1H; OH); elemental analysis calcd (%) for C₅₇H₆₆O₆·1.5H₂O: C 78.32, H 7.96; found C 78.41, H 8.15.

5,11,17,23-Tetra-tert-butyl-25-mono-[(6'-methoxynaphthalen-2'-yl)carbonylmethoxy]-26,27,28-tris-(ethoxycarbonylmethoxy)-calix[4]arene (3): Compound **2** (425 mg, 0.4 mmol) and ethyl bromoacetate (177 μL, 1.6 mmol) were refluxed in the presence of K₂CO₃ (123 mg, 0.8 mmol) in acetone (40 mL) for 12 h. The reaction mixture was filtered and concentrated under vacuum. The crude product was chromatographed on silica column (eluent CH₂Cl₂/AcOEt 80:20) and recrystallized from EtOH to give the desired product. Yield: 305 mg, 67%; m.p. 144 °C; ¹H NMR (400 MHz, CDCl₃): δ = 1.05 (m, 36H; tBu), 1.21 (m, 9H; CH₃), 3.21 (m, 4H; CH₂), 3.95 (s, 3H; CH₃), 4.1 (t, ²J(H,H) = 6 Hz, 4H), 4.15 (t, ²J(H,H) = 6 Hz, 2H), 4.81 (m, 8H), 5.05 (d, ²J(H,H) = 12 Hz, 2H), 5.72 (s, 2H), 6.82 (m, 8H), 7.15 (m, 2H), 7.72 (d, ²J(H,H) = 7.4 Hz, 1H; ArH), 7.91 (d, ²J(H,H) = 8.1 Hz, 1H; ArH), 8.07 (d, ²J(H,H) = 8 Hz, 1H; ArH), 8.59 (s, 1H; ArH); elemental analysis calcd (%) for C₆₉H₈₄O₁₂: C 74.97, H 7.66; found C 74.82, H 7.81.

5,11,17,23-Tetra-tert-butyl-25,26,27,28-tetra-[(6'-methoxynaphthalen-2'-yl)-carbonylmethoxy]calix[4]arene (4): 4-tert-Butylcalix[4]arene (505 mg, 0.77 mmol), K₂CO₃ (418 mg, 3.3 mmol), NaI (454 mg, 3.3 mmol) and 2-chloro-1-(6-methoxynaphthalen-2-yl)ethanone (710 mg, 3.3 mmol) in dry acetone were stirred under reflux under argon for 48 h. The reaction mixture was poured into water (50 mL) and extracted with dichloromethane. The extract was washed consecutively with 5% aqueous sodium metabisulfite, water, 3% sulfuric acid and water. The organic layer was dried over MgSO₄. The crude product was chromatographed on silica (eluent CH₂Cl₂/acetone 80:20) and recrystallized from MeOH to give the desired product. Yield: 280 mg, 34%; m.p. 152 °C; ¹H NMR (400 MHz, CDCl₃): δ = 1.21 (s, 36H; tBu), 3.52 (d, ²J(H,H) = 12 Hz, 4H; Ar-αCH_{ax}), 3.96 (s, 12H; OCH₃), 4.52 (d, ²J(H,H) = 12 Hz, 4H; Ar-αCH_{eq}), 5.49 (s, 4H; CH₂), 7.12 (d, ²J(H,H) = 8.8 Hz, 4H; ArH), 7.17 (s, 4H; ArH), 7.23 (m, 8H; ArH), 7.5 (d, ²J(H,H) = 9.2 Hz, 4H; ArH), 7.72 (m, 8H; ArH), 8.16 (s, 4H; ArH); ¹³C NMR (100.6 MHz, CDCl₃): δ = 30.2 (CH₂), 31.4 (CH₃), 34.3 (C(CH₃)₃), 55.6 (OCH₃), 79.1 (CH₂CO), 105.9 (CHAr), 120.1 (CHAr), 123.9 (CHAr), 126 (CHAr), 127.6 (CHAr), 129.2 (CAr), 129.4 (CHAr), 131.1 (CHAr), 134.6 (CAr), 137.9 (CAr), 148.5 (COAr), 150.4 (COAr),

160.2 (CArC=O), 195.6 (C=O); elemental analysis calcd (%) for C₉₇H₉₈O₁₂·3H₂O: C 77.16, H 6.94; found C 77.38, H 6.81.

Solvents and salts: Acetonitrile from Aldrich (spectrometric grade) and absolute ethanol from SDS (spectrometric grade) were used as solvents for absorption and fluorescence measurements. Alkali and alkaline-earth perchlorates and potassium thiocyanate, from Alfa, were of the highest quality available and vacuum dried over P₂O₅ prior to use.

Spectroscopic measurements and calculations: UV/vis absorption spectra were recorded on a Varian Cary5E spectrophotometer. Corrected emission spectra were obtained on a SLM-Aminco8000C spectrofluorimeter. The fluorescence quantum yields were determined by using quinine sulfate dihydrate in H₂SO₄ (0.1N) as a reference ($\Phi_F = 0.546$)^[12]. All solvents used were of spectroscopic grade.

Steady-state fluorescence anisotropies, defined as $r = (I_{\parallel} - I_{\perp}) / (I_{\parallel} + 2I_{\perp})$ (where I_{\parallel} and I_{\perp} are the fluorescence intensities observed with vertically polarized excitation light and vertically and horizontally polarized emissions, respectively) were determined by the G-factor method. Low temperature measurements (100 K) were carried out in specially made 1 cm × 1 cm strain-free quartz cuvettes and with an Oxford DN1704 cryostat with quartz windows.

The critical radius for transfer by the dipolar mechanism was evaluated from the following Equation:

$$R_0 = 0.020108 \left[\kappa^2 \phi_0 n^{-4} \int_0^{\infty} I(\lambda) \epsilon(\lambda) \lambda^4 d\lambda \right]^{1/6} \quad (5)$$

with R_0 in nm, where κ^2 is the orientational factor, ϕ_0 is the donor fluorescence quantum yield, n is the average refractive index of the medium in the wavelength range in which spectral overlap is significant, $I(\lambda)$ is the normalized fluorescence spectrum of the donor, $\epsilon(\lambda)$ is the acceptor absorption coefficient [dm³ mol⁻¹ cm⁻¹] and λ is the wavelength in nanometers. The orientation factor was taken to be equal to the dynamic average, that is $\frac{2}{3}$. The refractive index was chosen to be that of ethanol. Under these conditions, the value of R_0 calculated by Equation (5) is 0.8 nm.

Time-resolved fluorescence-intensity decays were obtained by the single-photon timing method, with picosecond laser excitation with a Spectra-Physics set-up composed of a Titanium Saphir Tsunami laser pumped by an argon ion laser, a pulse selector and doubling (LBO) and tripling (5BBO) crystals. Light pulses were selected by optoacoustic crystals at a repetition rate of 4 MHz. Fluorescence photons were detected by means of a Hamamatsu MCP R3809U photomultiplier, connected to a constant-fraction discriminator. The time-to-amplitude converter was purchased from Tennelec. In this investigation, the FWHM (full width at half maximum height) instrument response was 61 ps. Data were analysed by the maximum entropy method.^[26]

Transient absorption measurements were carried out by nanosecond laser flash photolysis. The instrument uses the third harmonics of a BM Industries Q-switched Nd-YAG (model BMI 5011 DNS 10), delivering 7–8 ns pulses at 1064 nm. Q-switching was achieved with a Pockels cell inside the cavity. The giant pulse was frequency-doubled and -tripled in potassium dihydrogen phosphate (KDP) crystals. The output energy was 120 mJ at 355 nm. The energy deposited in the sample was lowered to 3 mJ by interposing a diffusing plate in front of the irradiation cell. The excitation beam and the probe beam generated by a pulse xenon source were perpendicular to each other inside the 1 × 1 cm cell. The analysing beam was spectrally dispersed by a monochromator and converted into an electric signal by a Hamamatsu R 928 PM tube. The electrical signal was recorded by a digital memory oscilloscope (Tektronix TDS 620 B) connected to a PC. The transient signals were analysed by an Igor® procedure-based in-house routine. The reported decays and rate constants are the mean values of at least ten different measurements.

Energy-minimized structures were generated by Hyperchem V5.1 software with MM+ as force-field.

Global analysis of the evolution of the whole absorption spectra was performed with the Specfit Global Analysis System V3.0 for 32-bit Windows systems. This software uses singular value decomposition and nonlinear regression modelling by the Levenberg–Marquardt method.^[27]

Acknowledgement

We thank P. Denjean and Dr. R. Pansu for their assistance in tuning the single-photon timing instrument. F. O'Reilly, J.-L. Habib-Jiwan and J.-Ph. Soumillion are acknowledged for their help in the synthesis of Calix-AMN1.

- [1] *Fluorescent Chemosensors for Ion and Molecule Recognition* (Ed.: A. W. Czarnik), ACS Symposium **1993**, Series 358.
- [2] "Chemosensors of Ion and Molecule Recognition" (Eds.: J.-P. Desvergne, A. W. Czarnik), *NATO ASI Ser. C* **1997**, 492.
- [3] A. P. de Silva, H. Q. N. Gunaratne, T. Gunnlaugsson, A. J. M. Huxley, C. P. McCoy, J. T. Rademacher, T. E. Rice, *Chem. Rev.* **1997**, 97, 1515–1566.
- [4] L. Fabbrizzi, A. Poggi, *Chem. Soc. Rev.* **1995**, 24, 197–202.
- [5] B. Valeur, I. Leray, *Coord. Chem. Rev.* **2000**, 202, 3, 40.
- [6] a) V. Böhmer, *Angew. Chem.* **1995**, 107, 785–818; *Angew. Chem. Int. Ed. Engl.* **1995**, 34, 713–745; b) A. Ikeda, S. Shinkai, *Chem. Rev.* **1997**, 97, 1713–1734; c) D. Diamond, M. A. McKervey, *Chem. Soc. Rev.* **1996**, 15–24.
- [7] a) I. Aoki, T. Sakaki, S. Shinkai, *Chem. Commun.* **1992**, 730–731; b) F. Unob, Z. Asfari, J. Vicens, *Tetrahedron Lett.* **1998**, 39, 2951–2954; c) H. F. Ji, G. M. Brown, R. Dabestani, *Chem. Commun.* **1999**, 609–610; d) H. F. Ji, R. Dabestani, G. M. Brown, R. A. Sachleben, *Chem. Commun.* **2000**, 833–834; e) H. F. Ji, G. M. Brown, R. Dabestani, *J. Am. Chem. Soc.* **2000**, 122, 9306–9307.
- [8] a) I. Aoki, H. Kawabata, K. Nakashima, S. Shinkai, *Chem. Commun.* **1991**, 1771–1772; b) K. Iwamoto, K. Araki, H. Fujishima, S. Shinkai, *J. Chem. Soc. Perkin Trans. 1* **1992**, 1885–1887.
- [9] I. Leray, F. O'Reilly, J.-L. Habib-Jiwan, J.-Ph. Soumillion, B. Valeur, *Chem. Commun.* **1999**, 795–796.
- [10] a) T. Jin, K. Ichikawa, T. Koyama, *Chem. Commun.* **1992**, 499–500; b) M. Takahashi, S. Shinkai, *Chem. Lett.* **1994**, 125–128; c) T. Jin, K. Monde, *Chem. Commun.* **1998**, 1357–1358; T. Jin, K. Monde, *Chem. Commun.* **1998**, 122, 9306–9307; d) N. Van Der Veen, S. Flink, M. Deij, R. Egberink, F. Van Veggel, D. Reinhoudt, *J. Am. Chem. Soc.* **2000**, 122, 6112–6113.
- [11] T. Jin, *Chem. Commun.* **1999**, 2491–2492.
- [12] a) K. Crawford, M. Goldfinger, T. Swager, *J. Am. Chem. Soc.* **1998**, 120, 5817–5192; b) C. Perez-Jimenez, S. Harris, D. Diamond, *Chem. Commun.* **1993**, 480–481.
- [13] a) J. Bourson, M. N. Borrel, B. Valeur, *Anal. Chim. Acta* **1992**, 257, 189–193; b) J. Bourson, J. Pouget, B. Valeur, *J. Phys. Chem.* **1993**, 97, 4552–4557; c) J. Bourson, F. Badaoui, B. Valeur, *J. Fluorescence* **1994**, 4, 275–277; d) J.-L. Habib-Jiwan, C. Branger, J.-Ph. Soumillion, B. Valeur, *J. Photochem. Photobiol. A: Chem.* **1998**, 116, 127–133; e) I. Leray, J.-L. Habib-Jiwan, C. Branger, J.-Ph. Soumillion, B. Valeur, *J. Photochem. Photobiol. A: Chem.* **2000**, 135, 163–169.
- [14] F. Arnaud-Neu, E. M. Collins, M. Deasy, G. Ferguson, S. J. Harris, B. Kultner, A. J. Lough, M. A. McKervey, E. Marques, B. L. Rubl, M. J. Schwing-Weil, E. M. Seward, *J. Am. Chem. Soc.* **1989**, 111, 8681–8691.
- [15] a) V. Balzani, P. Ceroni, S. Gestermann, C. Kauffmann, M. Gorka, F. Vögtle, *Chem. Commun.* **2000**, 853–854; b) F. Vögtle, S. Gestermann, C. Kauffmann, P. Ceroni, V. Vicinelli, V. Balzani, *J. Am. Chem. Soc.* **2000**, 122, 10398–10404.
- [16] M. Balo, F. Fernandez, C. Gonzalez, E. Lens, C. Lopez, *J. Chem. Res. (S)* **1993**, 132–133.
- [17] T. Grady, S. Harris, M. Smyth, D. Diamond, *Anal. Chem.* **1986**, 68, 3775–3782.
- [18] M. N. Berberan-Santos, J. Canceill, J. C. Brochon, L. Jullien, J. M. Lehn, J. Pouget, P. Tauc, B. Valeur, *J. Am. Chem. Soc.* **1992**, 114, 6427–6436.
- [19] N. J. Turro, *Modern Molecular Photochemistry*, Benjamin, Melno Park (CA), **1978**.
- [20] D. Devapiriam, K. Rajasekaran, C. Gnanasekaran, *Spectrochimica Acta* **1992**, 48A, 835–838.
- [21] R. Nurmukhametov, L. Mileshina, D. Shigorin, *Opt. Spectrosc.* **1967**, 23, 404–407.
- [22] A. A. Lamola, *J. Chem. Phys.* **1967**, 47, 4810–4816.
- [23] N. C. Yang, D. S. McClure, S. L. Murov, J. J. Houser, R. Dusenbry, *J. Am. Chem. Soc.* **1967**, 89, 5466–5468.
- [24] a) M. N. Berberan-Santos, J. Pouget, B. Valeur, J. Canceill, L. Jullien, J. M. Lehn, *J. Phys. Chem.* **1993**, 97, 11376–11379; b) M. N. Berberan-Santos, P. Choppinet, A. Fedorov, L. Jullien, B. Valeur, *J. Am. Chem. Soc.* **2000**, 122, 11876–11886.
- [25] Y. Israeli, C. Detellier, *J. Phys. Chem. B* **1997**, 101, 1897–1901.
- [26] A. K. Livesey, J. C. Brochon, *Biophys. J.* **1987**, 52, 693–706.
- [27] H. Gampp, M. Maeder, C. J. Meyer, A. D. Zuberbühler, *Talanta* **1985**, 32, 95–101.

Received: March 2, 2001 [F3106]